JOURNAL OF COMPUTATIONAL PHYSICS 27, 88–102 (1978)

NEUCG: A Transport Code for Hydrogen Atoms in Cylindrical Hydrogenic Plasmas

KEITH H. BURRELL

General Atomic Company, San Diego, California 92138

Received January 3, 1977; revised May 2, 1977

A special code describing transport of neutral hydrogen atoms in a hydrogenic plasma has been written. Test comparisons with solutions based on a neutron transport code show that the accuracy is good and the execution time is improved by a factor of six. The code accepts arbitrary, smooth electron and ion density and temperature profiles. Maximum temperatures permitted for accurate results are about 5 keV.

1. INTRODUCTION

The interaction of neutral hydrogen atoms with the background hydrogenic plasmas is an important component in the physics of tokamak plasmas. These neutrals affect both the particle and energy balance of the plasma, providing a source of new plasma and a channel for cross field heat transport. In addition, hot neutrals which leave the plasma volume can interact with the wall of the plasma chamber, sputtering impurities into the plasma and (in reactors) possibly damaging the wall. Finally, these hot neutrals can also be used for plasma diagnostics. Accordingly, a description of neutral transport is of interest to surface physicists, plasma diagnosticians, and builders of plasma transport codes.

The problem of netural hydrogen transport is very similar to that of neutron and photon transport. Thus, at first glance, it would seem to require little work to adapt one of the latter codes to our present problem. (Indeed, this has been advocated [1] and is being carried out at Oak Ridge National Laboratory [2].) However, since such codes usually run as a complete program, rewriting them into a subroutine for a plasma transport code is not a trivial undertaking. More importantly, these codes tend to be rather slow, since they are designed to solve the Boltzmann transport equation including the complicated neutron collision terms. The neutral behavior is governed by very simple cross sections; consequently, one can create a much faster, more compact code by writing a special-purpose routine based on an integral transport equation. (According to Hogan's review of plasma codes [3], this do-it-yourself approach seems to have been taken by most fusion groups that have written plasma transport codes.)

A neutron transport code has, however, been used to check the results of the present work. The agreement is good, and the test runs confirm that the special-purpose code

0021-9991/78/0271-0088$02.00/0

is at least a factor of six faster. Since the neutral code is the slowest major element in the plasma transport code, this results in a significant improvement in execution time for that code.

At present, the code has the following features. Arbitrary smooth electron and ion density and temperature profiles are allowed. The calculation can be done for any hydrogen isotope. The code can calculate the neutral number density $n(r)$, the neutral average energy $w_n(r) = \langle mv^2 f(r, \mathbf{v})/3n(r)\rangle$ and the phase space distribution function at the plasma edge of those neutrals whose velocities are outwardly directed. The neutral interaction with the wall is modeled as a diffuse reflection in which the incoming neutral is assumed to thermally accommodate with the wall and thus to return at the wall temperature. The code is limited to electron and ion temperatures below about 5 keV by the assumptions made about the ionization rates.

The discussion of the code will be organized in the following manner. In Section 2, the integral equation will be obtained from the Boltzmann transport equation, while in Section 3, the methods used to program the discrete form of the integral equation will be discussed. Some of the programming methods used to speed execution are discussed in Section 4, while Section 5 closes the paper with a comparison of the results of the present code with a neutron transport code.

2. Integral Equation

To properly formulate the problem of neutral hydrogen transport, the Boltzmann equation must be used. The scale length of the background plasma can be shorter than the neutral mean-free paths for ionization and charge exchange, which makes a treatment based on the moment (fluid) equations questionable. [Such a treatment is especially poor for low density plasmas (10^{13} cm^{-3} density) in the smaller of present-day devices (dimensions 10 to 20 cm).]

Since present tokamak minor radii are tens of centimeters, and since the plasma transport time scale is milliseconds or longer, the steady-state Boltzmann equation is appropriate for the neutrals. Considering the cross sections given by Freeman and Jones [4], the dominant interactions for neutrals in hydrogen plasmas with electron and ion temperatures below about 5 keV are ionization by electron impact and charge exchange with ions. (We assume there are sufficiently few neutrals in the system that their self interactions can be neglected.) This leads to the following steady-state kinetic equation

$$\mathbf{v} \cdot \nabla f(\mathbf{x}, \mathbf{v}) = -\int |\mathbf{v} - \mathbf{v}'| \, \sigma_{en} f_e(\mathbf{x}, \mathbf{v}') f(\mathbf{x}, \mathbf{v}) \, d^3\mathbf{v}' + \int |\mathbf{v} - \mathbf{v}'| \, \sigma_{cx} [f(\mathbf{x}, \mathbf{v}') f_i(\mathbf{x}, \mathbf{v}) - f(\mathbf{x}, \mathbf{v}) f_i(\mathbf{x}, \mathbf{v}')] \, d^3\mathbf{v}' \qquad (1)$$

where f, f_e, and f_i are the neutral, electron, and ion distribution functions, respectively, and σ_{en} and σ_{cx} are electron ionization and charge exchange cross sections, respectively.

In principle, the right-hand side of Eq. (1) should also include terms describing the interaction of the neutral atoms with the other ions that may occur in the plasma (e.g., oxygen, carbon, etc.). Charge exchange is the most important of these. Unfortunately, there are no cross sections available for charge exchange with highly stripped ions in the energy range of interest for present-day machines ($E \lesssim 1$ keV). Thus, in the absence of knowledge, these terms were left out.

For roughly equal energies, the electrons have much greater speeds than the neutrals. Accordingly, the ionization rate coefficient, α, is independent of neutral velocity. In addition, as given in Freeman and Jones [4], $v\sigma_{cx}(v)$ is a slowly varying function of energy $E = mv^2/2$ for $E \leqslant 20$ keV. Consequently, it will be taken to be a constant C. Under these assumptions, Eq. (1) becomes

$$\mathbf{v} \cdot \nabla f(\mathbf{x}, \mathbf{v}) = -A(\mathbf{x}) f(\mathbf{x}, \mathbf{v}) + B(\mathbf{x}) F(\mathbf{x}, \mathbf{v}) n(\mathbf{x}) \tag{2}$$

where $A(\mathbf{x}) = n_e(\mathbf{x})\, \alpha(\mathbf{x})$; $B(\mathbf{x}) = n_i(\mathbf{x})C$; and $n(\mathbf{x})$, $n_e(\mathbf{x})$, and $n_i(\mathbf{x})$ are the neutral, electron, and ion number densities, respectively. Here, $F(\mathbf{x}, \mathbf{v})$ is the ion velocity distribution function normalized to unity, i.e., $\int d^3\mathbf{v} F(\mathbf{x}, \mathbf{v}) = 1$.

The approximations of the cross sections are fundamental to the method used here. Since the reaction rates are the same for each neutral, regardless of its velocity, it is not surprising that it is possible to reduce Eq. (2) to an integral equation for neutral number density. (These approximations are not new; they have been used at least twice before [5, 6].)

We will assume that the plasma looks like an infinitely long cylinder of radius a, and we will take $A(\mathbf{x})$, $B(\mathbf{x})$, and $F(\mathbf{x}, \mathbf{v})$ to be functions only of radius. Accordingly, the effects of poloidal curvature of the plasma will be properly handled, but variations due to toroidal curvature will not be.

It is now convenient to transform the differential operator in Eq. (2) into cylindrical coordinates. Taking advantage of the cylindrical symmetry and axial invariance, we find [7]

$$\mathbf{v} \cdot \nabla f = v_r \cos\omega \frac{\partial f}{\partial r} - \frac{v_r}{r} \sin\omega \frac{\partial f}{\partial \omega} \tag{3}$$

where $r = (x^2 + y^2)^{1/2}$, $\omega = \tan^{-1}(v_y/v_x) - \tan^{-1}(x/y)$, $v_r = (v_x^2 + v_y^2)^{1/2}$. Here (x, y, z) and (v_x, v_y, v_z) are the usual cartesian coordinates and velocity components, respectively. From now on, we will think of $f = f(r, \omega, v_r, v_z)$.

Before Eq. (2) can be uniquely integrated, we must specify boundary conditions. Unfortunately, there is a lack of experimentally measured neutral reflection coefficients for surfaces and energy ranges of interest. Consequently, the simplest boundary condition that meets the intuitive requirements has been chosen, the so-called diffuse reflection condition,

$$f(a, \omega, v_r, v_z) = f_0(\mathbf{v}) + R_D h_0(\mathbf{v})\, \Gamma_+(f), \qquad \frac{\pi}{2} \leqslant \omega \leqslant \frac{3\pi}{2} \tag{4}$$

where $f_0(\mathbf{v})$ and $h_0(\mathbf{v})$ are given distribution functions and where $\Gamma_+(f)$ is the one-sided radial flux,

$$\Gamma_+(f) = \int_0^\infty dv_r \int_{-\infty}^{+\infty} dv_z \int_{-\pi/2}^{\pi/2} d\omega \, v_r^2 \cos\omega f(a, \omega, v_r, v_z). \tag{5}$$

We flux normalize $h_0(v)$ so that

$$\int_0^\infty dv_r \int_{-\infty}^{+\infty} dv_z \int_{\pi/2}^{3\pi/2} d\omega \, v_r^2 \cos\omega h_0(\mathbf{v}) = -1. \tag{6}$$

In Eq. (4), the distribution function $f_0(\mathbf{v})$ represents the neutral source on the wall due to plasma that is recombining there, while the other term models neutral collisions with the wall. In general, neutral–wall collisions in this model do not conserve particles or energy. By choosing $R_D = 1$, particle conservation is assured. Since neutrals generally lose energy on collision, we do not require an energy conserving model.

Notice that Eq. (4) is a linear superposition of two known source terms, f_0 and h_0. Only the coefficient $\Gamma_+(f)$ is unknown. Since Eq. (2) is linear in $f(\mathbf{x}, \mathbf{v})$, we will solve Eqs. (2) and (4) for a fixed $R_D \neq 0$ by first solving two problems with $R_D = 0$ (one for each source term), and then taking the proper superposition of the two solutions.

We can obtain the integral equation from Eqs. (2) and (4) in the manner shown in Appendix A. The result for general $f_0(\mathbf{v})$ and $F(r, \mathbf{v})$ is given there; the case that is of most interest is when these distribution functions are Maxwellian. For this latter case, we find

$$n(r) = h(r) + \int_0^a d\rho \, K(\rho, r) \, n(\rho) \tag{7}$$

where

$$h(r) = \frac{2n_0}{\sqrt{\pi}} \int_0^{\pi/2} d\omega \left[G_1\left(\frac{A_+(a, r, \omega)}{v_W}\right) + G_1\left(\frac{A_-(a, r, \omega)}{v_W}\right)\right], \tag{8}$$

$$K(\rho, r) = \frac{\rho B(\rho)}{\sqrt{\pi}\, v_{th}(\rho)} \int_0^{\pi/2} \frac{d\theta}{(\rho_>^2 - \rho_<^2 \sin^2\theta)^{1/2}} \times \left[G_0\left(\frac{A_+(\rho_>, \rho_<, \theta)}{v_{th}(\rho)}\right) + G_0\left(\frac{A_-(\rho_>, \rho_<, \theta)}{v_{th}(\rho)}\right)\right], \tag{9}$$

$$\rho_> = \max(\rho, r), \qquad \rho_< = \min(\rho, r),$$

$$A_\pm(\rho_>, \rho_<, \theta) = | A_T[(\rho_>^2 - \rho_<^2 \sin^2\theta)^{1/2}, \rho_< \sin\theta] \pm A_T(\rho_< \cos\theta, \rho_< \sin\theta)|, \tag{10}$$

$$A_T(x, y) = \int_0^x d\xi \, A[(\xi^2 + y^2)^{1/2}], \tag{11}$$

$$G_n(x) = \frac{2}{\sqrt{\pi}} \int_0^\infty d\eta \, \eta^n \exp(-\eta^2 - x/\eta). \tag{12}$$

Here, the velocities v_W and $v_{th}(r)$ are the thermal velocities in $f_0(\mathbf{v})$ and $F(r, \mathbf{v})$, respec-

tively. The factor n_0 is the density of neutrals associated with the source term $f_0(\mathbf{v})$. It can be determined from the equation

$$\frac{n_0}{\sqrt{\pi}} = \frac{\Gamma_p}{v_W} + \frac{n_b}{\sqrt{\pi}}, \tag{13}$$

where Γ_p is the outgoing plasma flux at the wall and represents plasma recombination while n_b is any additional background neutral density that the user wishes to specify.

The numerical solution of the problem posed by Eqs. (7)–(13) is the subject of the next section. Here we wish to conclude by indicating how one can obtain other quantities of interest once $n(r)$ is known.

For those who work with plasma transport codes, the average neutral energy is of interest. This is the term that appears in the ion-neutral energy exchange term and is defined as

$$w_n(r) \equiv \frac{m}{3n(r)} \langle v^2 f(r, \mathbf{v}) \rangle. \tag{14}$$

Using the form for $f(r, \mathbf{v})$ found in Appendix A, a straightforward calculation yields

$$w_n(r) = \frac{1}{3} T_i(r) + \frac{1}{3n(r)} \left\{ [T_W - T_i(r)]\, h(r) + \frac{2}{3} T_W h_T(r) + \frac{2}{3} \int_0^a d\rho\, K_T(\rho, r)\, n(\rho)\, T_i(\rho) \right\} \tag{15}$$

where $T_i(r) = mv_{th}^2(r)/2$ and $T_W = mv_W^2/2$. The functions $h_T(r)$ and $K_T(\rho, r)$ are identical in form to $h(r)$ and $K(\rho, r)$ except that the G_1's and G_0's are replaced by G_3's and G_2's, respectively.

For plasma diagnostics and surface physics applications, one also wishes to know the distribution function of outgoing neutrals at the wall. This is given by

$$f(a, \omega, v_r, v_z) = f_0(v_r, v_z) \exp\left[-\frac{2}{v_r} A_T(r_1, r_0) \right] + \int_0^{r_1} d\xi \left(\exp\left\{ -\frac{1}{v_r} [A_T(r_1, r_0) - A_T(\xi, r_0)] \right\} + \exp\left\{ -\frac{1}{v_r} [A_T(r_1, r_0) + A_T(\xi, r_0)] \right\} \right) \times \frac{B[\rho(\xi)]}{v_r} F(\rho(\xi), v_r, v_z)\, n[\rho(\xi)] \tag{16}$$

where $\rho(\xi) = (\xi^2 + a^2 \sin^2 \omega)^{1/2}$, $r_1 = a \cos \omega$, and $r_0 = a \sin \omega$.

Thus, we have shown that the original Boltzmann transport equation can be reduced, in this case, to a one-dimensional integral equation. This eases the numerical problem considerably, since we seek $n(r)$ instead of $f(r, \mathbf{v})$. Once $n(r)$ is known, any

quantity of interest can be computed by evaluating the appropriate integral. As mentioned previously, this great simplication would not have been possible without the assumptions made about the rate coefficients α and C.

3. Discrete Approximations

For numerical work, the integral equation (7) must be written as a matrix equation by approximating the integral as a sum by means of a mechanical quadrature. If n abscissas are used in the quadrature, the work necessary to evaluate $K(\rho, r)$ scales as n^2. Consequently, it behooves us to choose a Gaussian quadrature [8], since this gives the best accuracy for the fewest number of base points.

Gaussian quadrature formulas do not, of course, have equally spaced abscissas. Accordingly, the internal base points in the code will not correspond in general to the grid points used, for example, in the plasma transport code. Input quantities such as electron and ion densities and temperatures will have to be interpolated to find their values at the internal base points; after the solution is complete another interpolation will be necessary to find neutral density and average energy values at the external points. However, this is a small price to pay for the great savings in execution time that a reduction in n brings. (In a slab geometry neutral code that I have written, changing from trapezoidal rule to Gaussian quadratures reduced execution time by a factor of 10.)

Most Gaussian quadratures use base points internal to the interval of integration. This is inconvenient, since we wish to know quantities such as $n(0)$ or $n(a)$. For this reason, a Lobatto quadrature [8] was chosen, which uses the endpoints of the interval as two of the base points.

Unfortunately, due to the behavior of $K(\rho, r)$ as $\rho \to r$, we cannot simply substitute the quadrature sum for the integral in Eq. (7). Analysis of the expression in Eq. (9) for the kernel $K(\rho, r)$ shows it to have a logarithmic singularity in the limit $\rho \to r$. To cope with this problem, Eq. (7) can be modified to read

$$n(r)\left[1 - \int_0^a d\rho\, K(r, \rho)\right] = h(r) + \int_0^a d\rho\, [K(\rho, r)\, n(\rho) - K(r, \rho)\, n(r)]. \tag{17}$$

The integral on the right-hand side is now well behaved and the Lobatto quadrature can be applied in a straightforward manner. The integral on the left-hand side can be done using quadrature formulas developed by Krylov and Paltsev [9]. (The appearance of the unknown function $n(\rho)$ in the integrand in Eq. (7) makes it difficult to apply these latter formulas to that integral directly.)

The discrete form for Eq. (7) can now be written as

$$n(r_i)\left[1 - I(r_i) + \sum_{j \neq i} w_j K(r_i, r_j)\right] = h(r_i) + \sum_{j \neq i} w_j K(r_j, r_i)\, n(r_j) \tag{18}$$

where r_i and w_i $(i = 1, 2, \ldots, n)$ are the abscissas and weights for the Lobatto quadrature and where

$$I(r) = \int_0^a d\rho\, K(r, \rho). \tag{19}$$

Having obtained the matrix form in Eq. (18), we now seek to solve for $n(r_i)$. This could be done by direct elimination, since the usual value of n is 22. However, to preclude problems with roundoff, an iterative solution method, normalized Gauss-Seidel iteration, was chosen. This is similar to the usual Gauss-Seidel method [10], but after each complete iteration, the new solution vector $n(r_i)$ is multiplied by a constant that insures particle conservation. This should speed up convergence. (See Honeck [11] for tests of an analogous scheme.) The detailed derivation of the conservation integral is given in Appendix B. Since the calculation of the matrix $K(r_i, r_j)$ essentially determines the execution time, this refinement of renormalizing is perhaps not really necessary.

As was mentioned in the previous section, the numerical solution first obtained is that appropriate for a system with $R_D = 0$. We now wish to effect the linear superposition that leads to the complete solution. This is particularly easy at present, since $h_0(\mathbf{v})$ in Eq. (4) is taken to be proportional to $f_0(\mathbf{v})$. This means that the $R_D = 0$ solution and the $R_D \neq 0$ solution simply differ by a constant factor, which can be determined from Eq. (4). For the case that $f_0(\mathbf{v})$ and $F(r, \mathbf{v})$ are Maxwellian, a straightforward calculation gives the constant factor γ to be

$$\gamma = (1 - R_D C_1)^{-1} \tag{20}$$

where

$$\begin{aligned} C_1 = {} & 2\int_0^{\pi/2} d\omega \cos\omega G_2\left(\frac{2A_T(r_1, r_0)}{v_W}\right) \\ & + \frac{2}{n_0 a v_W}\int_0^a d\rho\, \rho B(\rho)\, n(\rho) \int_0^{\pi/2} d\theta \\ & \times \left[G_1\left(\frac{A_+(a, \rho, \theta)}{v_{th}(\rho)}\right) + G_1\left(\frac{A_-(a, \rho, \theta)}{v_{th}(\rho)}\right)\right]. \end{aligned} \tag{21}$$

The original solution must be multiplied by γ to become the $R_D \neq 0$ solution.

Solutions for the cases with $h_0(\mathbf{v})$ different from $f_0(\mathbf{v})$ would run almost as rapidly as the present one, since the iterative solution is much faster than evaluating $K(r_i, r_j)$. However, in the absence of information on what $h_0(\mathbf{v})$ should be, the simpler path was chosen.

4. Programming Considerations

As is obvious from the definition of $K(\rho, r)$ in Eqs. (9)–(12), efforts to compute $A_T(x, y)$ and $G_n(x)$ as rapidly as possible will be well repaid. Each of these functions must be called roughly ten thousand times to evaluate the $K(r_i, r_j)$ matrix.

Since $G_n(x)$ is a real function of a real variable, it is quite amenable to the usual approximation techniques. Quick, accurate polynomial and rational Chebyshev approximations have been developed using the techniques given by Cody *et al.* [12]. These are used for $0 \leqslant x \leqslant 10$, while the asymptotic expansion [13] is used for larger values.

As a function of two variables that is also implicitly dependent on the electron and ion density and temperature profiles, the calculation of $A_T(x, y)$ appears to be much more difficult. Actually, that very dependence on the physical parameters can be made the basis of a fast algorithm by taking advantage of the fact that $A(r)$ is a smooth function of r. Accordingly, it is reasonable to approximate it as a power series in r

$$A(r) = \sum_{n=0}^{m} a_n r^{2n}. \tag{22}$$

Only even powers are necessary since the electron and ion densities and temperatures are cylindrically symmetric.

With this representation, we may write

$$A_T[(\rho^2 - r_0^2)^{1/2}, r_0] = \sum_{n=0}^{m} a_n r_0^{2n+1} b_n(\rho/r_0). \tag{23}$$

The b_n satisfy the convenient recursion relation

$$r_0^{2n+1} b_n = (2n + 1)^{-1}[(\rho^2 - r_0^2)^{1/2}\, \rho^{2n} + 2n r_0^2 \cdot r_0^{2(n-1)+1} b_{n-1}]. \tag{24}$$

When the program is first called, the a_n are evaluated (typically, ten are used); then, whenever $A_\pm$ are required, Eqs. (23) and (24) are used to find the corresponding A_T's.

Because of our assumption that $A(r)$ can be approximated by a polynomial, the present version of NEUCG will not work properly when $A(r)$ varies too rapidly as, for example, it would if $n_e(r)$ or $n_i(r)$ were step functions. Caution should be exercised in attempting to run such cases. However, any $n_e(r)$ and $n_i(r)$ smooth enough to be properly approximated on the 100 point grid typically used in plasma transport codes should not pose any problem for the $A(r)$ and $A_T(x, y)$ algorithms.

The method for calculating the ionization rate α and charge exchange rate C should also be mentioned. The fits to the Maxwellian rate coefficients developed by Freeman and Jones [4] are used. Notice that $\alpha = \alpha(T_e(r))$ while $C = C(T_i(r))$. By allowing C to depend on T_i, we rectify some of the error that our original approximation of $v\sigma_{cx}(v) =$ constant may have caused.

One final point needs to be made. At present, the code will only handle the problem of one hydrogen isotope moving through a plasma whose ions are of the same isotope. Thus, tritium transport in a tritium plasma will be properly calculation, but tritium in a deuterium plasma will not be.

5. Test Runs of Neucg

Comparisons runs were made on a UNIVAC 1110 and a DEC-10 to search for differences between the answers from NEUCG and the neutron transport code

DTFX, a variant of DTF-IV [14]. DTFX is a multigroup, discrete ordinates neutron transport code. The results for $n(r)$ and $w_n(r)$ are shown in Figs. 1 through 3 for various plasma density and temperature profiles. For these cases, the DTFX runs used the same $v\sigma_{cx}(v) = C(T_i)$ assumption that is used in NEUCG. The agreement between the results of the two codes is quite good, with the agreement for $n(r)$ being better than 10% on the average while that for $w_n(r)$ is better than 5%.

In the uniform plasma temperature cases in Figs. 1 and 2, the execution time for DTFX is about three times that for NEUCG. In the nonuniform temperature case of Fig. 3, which is more similar to the plasma transport code environment, DTFX is

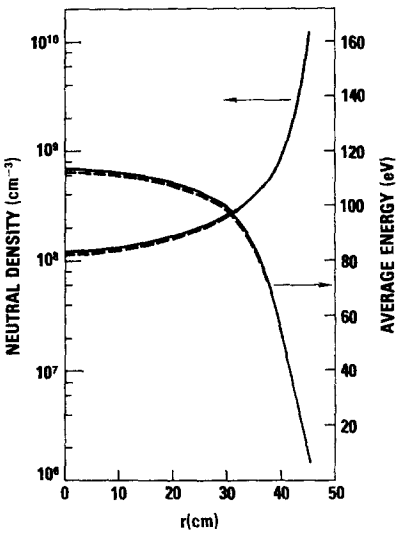

FIG. 1. Neutral density and average energy as calculated by NEUCG (solid line) and DTFX (dashed line) for the case $n_e = n_i = 10^{13}$ cm^{-3}, $T_e = T_i = 100$ eV, $T_w = 1$ eV, $\Gamma_p = 10^{16}$ cm^{-2} sec^{-1}, and $R_D = 0$. Plasma radius a is 45 cm.

about a factor of 6 slower. Accordingly, the present code represents a significant savings in execution time. In addition, although studies were made to optimize the number of spatial intervals, energy, and angular groups used, DTFX still required 55K storage on the UNIVAC-1110 for the case shown in Fig. 3. For the same case and machine, NEUCG used 6K.

It is interesting to note that the $w_n(r)$ profile in Figs. 1 and 2 show that it is possible to have $w_n > T_i$. In other words, in this case the neutrals would cool the ions at the edge, but heat them in the center. This is not what one would first expect. It is caused by the fact that the plasma acts as a velocity filter, i.e., those particles with higher speeds travel farther. Accordingly, the neutral population near $r = 0$ is enriched in high energy particles, causing the rise in w_n. However, this rise in w_n is not too fast, for we see in Fig. 3 that $w_n(r) < T_i(r)$. Since Fig. 3 is closer to the real tokamak case,

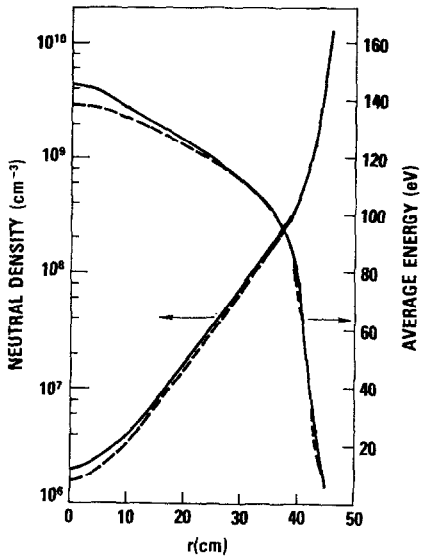

FIG. 2. Plots as in Fig. 1 but for $n_e = n_i = (5 - 4\,r^2/a^2) \times 10^{13}\,\mathrm{cm}^{-3}$. All other parameters are those of Fig. 1.

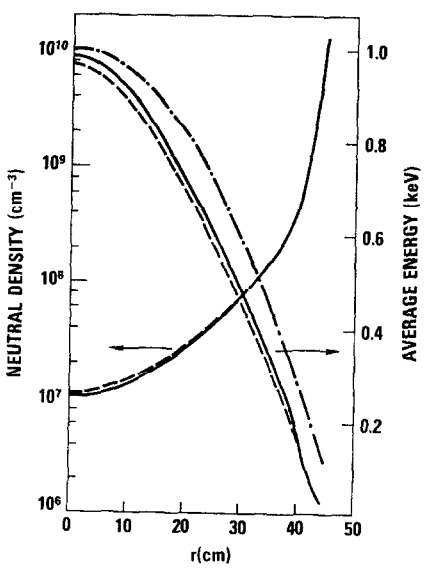

FIG. 3. Plots as in Fig. 1 but for $n_e = n_i = (5 - 4\,r^2/a^2) \times 10^{13}\,\mathrm{cm}^{-3}$ and $T_e = T_i = (1.0 - 0.9\,r^2/a^2)$ keV. All other parameters are those of Fig. 1. Also shown is the plasma temperature (dot-dashed lines).

it will probably be the case that the neutrals usually cool the ions. However, it is possible for the neutrals to locally heat the ions.

In Fig. 4, examples are given of the code option which returns the distribution function of outgoing neutrals at the plasma edge. The code will evaluate the distribution function $f(a, \mathbf{v})$ at various values of $\mathbf{v}$ specified by

$$v_x = v \sin\theta \cos\phi,$$
$$v_y = v \sin\theta \sin\phi,$$
$$v_z = v \cos\theta,$$

where $v = (2E/m)^{1/2}$, and E is the particle energy. Knowing this, one can calculate the neutral flux per unit energy per unit solid angle as is shown in the figures.

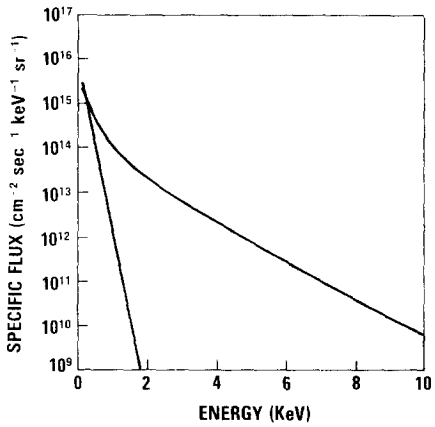

FIG. 4. Plot of the specific flux (flux/unit energy/unit solid angle) versus particle energy for the case in Fig. 2 (left-hand curve) and in Fig. 3 (right-hand curve). The flux is evaluated at the surface of the plasma for those particles whose velocity is normal to the surface.

Employing the true cross section for charge exchange, Pfeiffer [15] has made calculations using DTFX to investigate how large an error is produced by our approximation of that cross section. He has found that the $n(r)$ values in the outer portion of the plasma agree quite well while those in the center may be off by a factor of two at worst. Hence, in the region where the neutrals are relatively numerous, the present code does an adequate job of calculating their behavior.

APPENDIX A

In this section, the actual analysis leading from the Boltzmann transport equation to the integral equation for $n(r)$ will be carried out. The derivation is similar to others used to obtain the integral transport equation [16]; however, since the reaction

rates in this problem are independent of the neutral velocity, the final answer can be cast in a simpler form. The derivation is done using velocity variables, rather than energy and angle variables [16], since the invariance in the z direction makes v_z an ignorable coordinate, thus simplifying the computation.

Combining Eqs. (2) and (3) in the text, the equation we wish to integrate is

$$v_r \cos\omega \frac{\partial f}{\partial r} - \frac{v_r}{r} \sin\omega \frac{\partial f}{\partial \omega} = -A(r) f(r, \omega, v_r, v_z) + B(r) F(r, \mathbf{v}) n(r). \quad \text{(A.1)}$$

The boundary condition of interest is

$$f(a, \omega, v_r, v_z) = f_0(\mathbf{v}), \qquad \pi/2 \leqslant \omega \leqslant 3\pi/2. \quad \text{(A.2)}$$

To effect the integration, we need to use the characteristic coordinates of the differential operator in Eq. (A.1). These are

$$\begin{aligned} X &= r\cos\omega, \\ Y &= r\sin\omega. \end{aligned} \quad \text{(A.3)}$$

They transform the left-hand side of Eq. (A.1) to $v_r\, \partial f/\partial X$. For simplicity, we will assume that $f_0(\mathbf{v})$ and $F(r, \mathbf{v})$ are independent of ω.

Integrating Eq. (A.1), and employing Eq. (A.2), we have

$$\begin{aligned} f(X, Y, v_r, v_z) = f_0(\mathbf{v}) \exp\left\{-\frac{1}{v_r}\int_{-(a^2-Y^2)^{1/2}}^{X} d\xi\, A[\rho(\xi, Y)]\right\} \\ + \int_{-(a^2-Y^2)^{1/2}}^{X} d\xi \exp\left\{-\frac{1}{v_r}\int_{\xi}^{X} dl\, A[\rho(l, Y)]\right\} \frac{B[\rho(\xi, Y)]}{v_r} \\ \times F(\rho(\xi, Y), v_r, v_z)\, n[\rho(\xi, Y)] \end{aligned} \quad \text{(A.4)}$$

where

$$\rho(\xi, Y) = (\xi^2 + Y^2)^{1/2}.$$

In Eq. (A.4) we have an important intermediate step in our derivation. This equation will allow us to calculate the neutral distribution function once $n(r)$ is known. Consequently, we can find any moment of the distribution function that we require.

We now wish to integrate Eq. (A.4) over the velocity variables to obtain the integral equation. First we will perform the ω integral. Employing the symmetry in ω, we find

$$\int_0^{2\pi} d\omega\, f(r, \omega, v_r, v_z) = 2\int_0^{\pi/2} d\omega\, [f(X, Y, v_r, v_z) + f(-X, Y, v_r, v_z)]$$

$$= 2f_0(v_r, v_z)\int_0^{\pi/2} d\omega \exp\left\{-\frac{1}{v_r} A_T[(a^2 - Y^2)^{1/2}, Y]\right\}$$

$$\times \left\{\exp\left[\frac{1}{v_r} A_T(X, Y)\right] + \exp\left[-\frac{1}{v_r} A_T(X, Y)\right]\right\}$$

$$+ 2\int_0^{\pi/2} d\omega \int_{-(a^2-Y^2)^{1/2}}^{(a^2-Y^2)^{1/2}} d\xi \exp\left[-\frac{1}{v_r} |A_T(X, Y) - A_T(\xi, Y)|\right]$$

$$\times \frac{B[\rho(\xi, Y)]}{v_r} F(\rho(\xi, Y), v_r, v_z)\, n[\rho(\xi, Y)] \tag{A.5}$$

where $A_T(X, Y)$ is defined in Eq. (11) in the main text.

We now perform the following changes of variable in the second integral in Eq. (A.5). First, using the symmetry in ξ and the definition $\rho = (\xi^2 + Y^2)^{1/2}$, convert the ξ integral to one over ρ. Then make the substitution $r \sin \omega = \rho_< \sin \theta$ in the ω integral and exchange the order of θ and ρ integrals, taking care to put the proper limits on each. (The quantity $\rho_<$ is defined in Eq. (9).) After this, we may integrate over v_r and v_z to finally obtain

$$n(r) = 2\int_0^\infty v_r\, dv_r f_0(v_r) \int_0^{\pi/2} d\omega \left\{\exp\left[-\frac{A_+(a, r, \omega)}{v_r}\right]\right.$$

$$\left. + \exp\left[-\frac{A_-(a, r, \omega)}{v_r}\right]\right\} + 2\int_0^a d\rho\, \rho B(\rho)\, n(\rho) \int_0^\infty dv_r\, F(\rho, v_r)$$

$$\times \int_0^{\pi/2} \frac{d\theta}{(\rho_>^2 - \rho_<^2 \sin^2\theta)^{1/2}} \left\{\exp\left[-\frac{A_+(\rho_>, \rho_<, \theta)}{v_r}\right]\right.$$

$$\left. + \exp\left[-\frac{A_-(\rho_>, \rho_<, \theta)}{v_r}\right]\right\} \tag{A.6}$$

where $A_\pm$ are defined in Eq. (10) and $f_0(v_r)$ and $F(\rho, v_r)$ are $f_0(v_r, v_z)$ and $F(\rho, v_r, v_z)$ integrated over v_z.

Equation (A.6) is the result we were seeking. To further simplify the integrals, forms for $f_0(v_r)$ and $F(\rho, v_r)$ must be chosen. When these are Maxwellian, the main text results are obtained.

Appendix B

The normalization step in the normalized Gauss-Seidel iteration adjusts the trial solution to insure particle conservation. The basic conservation equation is

$$a\Gamma(a) = -\int_0^a d\rho\, \rho n_e(\rho)\, \alpha(\rho)\, n(\rho) \tag{B.1}$$

where $\Gamma(a)$ is the neutral flux at $r = a$. This is, of course, just the integrated form of the continuity equation.

$\Gamma(a)$ is the net flux, the difference of the inward going (Γ_-) and outward going (Γ_+) single-sided fluxes. For the case $R_D = 0$, we have for the first

$$\Gamma_- = -\int_0^\infty v_r^2\, dv_r \int_{-\infty}^{+\infty} dv_z \int_{\pi/2}^{3\pi/2} d\omega \cos\omega f_0(v_r, v_z)$$

$$= 2\int_0^\infty dv_r\, v_r^2 f_0(v_r) \tag{B.2}$$

while the second is given by

$$\Gamma_+ = 2\int_0^\infty dv_r\, v_r^2 \int_{-\infty}^{+\infty} dv_z \int_0^{\pi/2} d\omega\, f(a, \omega, v_r, v_z) \cos\omega. \tag{B.3}$$

Employing the form for f from Eq. (A.4) and using the same changes of variables as were used to obtain Eq. (A.6), we may express Γ_+ in terms of integrals over $n(r)$ and $f_0(v_r)$. Consequently, Eq. (B.1) can be rewritten as

$$\frac{2}{a}\int_0^a d\rho\, \rho B(\rho)\, n(\rho) \int_0^\infty dv_r\, v_r F(\rho, v_r) \int_0^{\pi/2} d\theta \left\{\exp\left[-\frac{A_+(a, \rho, \theta)}{v_r}\right] + \exp\left[-\frac{A_-(a, \rho, \theta)}{v_r}\right]\right\} + \frac{1}{a}\int_0^a d\rho\, \rho n_e(\rho)\, \alpha(\rho)\, n(\rho)$$

$$= 2\int_0^\infty dv_r\, v_r^2 f_0(v_r) \left\{1 - \int_0^{\pi/2} d\omega \cos\omega \exp\left[-\frac{A_+(a, a, \omega)}{v_r}\right]\right\}. \tag{B.4}$$

Notice that the right-hand side of Eq. (B.4) is independent of $n(r)$ while the left depends on integrals over it. Any trial solution $n_*(r)$ can be renormalized to conserve particles by calculating the left- and right-hand sides of Eq. (B.4) separately and then multiplying $n_*(r)$ by the factor needed to make them equal.

For the case considered in the code where $f_0(\mathbf{v})$ and $F(r, \mathbf{v})$ are Maxwellian, Eq. (B.4) reduces to

$$\frac{1}{a}\int_0^a d\rho\, \frac{\rho B(\rho)}{\sqrt{\pi}}\, n(\rho) \int_0^{\pi/2} d\theta \left[G_1\left(\frac{A_+(a, \rho, \theta)}{v_r}\right) + G_1\left(\frac{A_-(a, \rho, \theta)}{v_r}\right)\right] + \frac{1}{a}\int_0^a d\rho\, \rho n_e(\rho)\, \alpha(\rho)\, n(\rho)$$

$$= \frac{n_0 v_W}{2\sqrt{\pi}}\left[1 - 2\int_0^{\pi/2} d\omega \cos\omega G_2\left(\frac{A_+(a, a, \omega)}{v_W}\right)\right]. \tag{B.5}$$

Performing the ρ integrals in Eq. (B.5) by Lobatto quadrature is straightforward, since both integrands are well-behaved.

ACKNOWLEDGMENTS

I would like to thank R. E. Waltz for his help in checking the derivation of Eqs. (7)–(12) for algebraic blunders. I am indebted to W. Pfeiffer for providing an interface with DTFX and for explaining the neutron transport formulation of the problem. I acknowledge use in NEUCG of several routines from the International Mathematical and Statistical Library.

This work was supported by the U. S. Energy Research and Development Administration under Contract No. E(04-3)-167, Project Agreement No. 38.

REFERENCES

1. E. GREENSPAN, *Nucl. Fusion* **14** (1974), 771.
2. E. C. CRUME, private communication.
3. J. T. HOGAN, "Methods of Computational Physics" (J. Killeen, Ed.), Vol. 16, Academic Press, New York, 1976.
4. R. L. FREEMAN AND E. M. JONES, "Atomic Collision Processes in Plasma Physics Experiments," Culham Laboratory Report CLM-R 137.
5. S. REHKER AND H. WOBIG, *Plasma Phys.* **15** (1973), 1083.
6. J. T. HOGAN, private communication.
7. D. W. DRAWBAUGH, *Nucl. Sci. Eng.* **44** (1971), 58.
8. A. H. STROUD AND D. SECREST, "Gaussian Quadrature Formulas," Prentice–Hall, Englewood Cliffs, N. J., 1966.
9. V. I. KRYLOV AND A. A. PALTSEV, "Tables for Numerical Integration of Functions with Logarithmic and Power Singularities," (Israel Program for Scientific Translation), Keter Press, Jerusalem, 1971.
10. E. ISAACSON AND H. B. KELLER, "Analysis of Numerical Methods," Chap. 1, Wiley, New York, 1966.
11. H. C. HONEK, *Nucl. Sci. Eng.* **8** (1960), 193.
12. W. J. CODY, W. FRASER, AND J. F. HART, *Numer. Math.* **12** (1968), 242.
13. I. A. STEGUN, Miscellaneous functions, *in* "Handbook of Mathematic Functions" (M. Abramowitz and I. A. Stegun, Eds.), Chap. 27, p. 1001, U. S. Government Printing Office, Washington, D.C., 1964.
14. K. D. LATHROP, "DTF-IV, A FORTRAN-IV Program for Solving the Multigroup Transport Equation with Anisotropic Scattering," Los Alamos Report LA-3373, 1976.
15. W. PFEIFFER, "Calculation of Neutral Transport in a Plasma Using a Neutron Transport Method," General Atomic Co. Report GA-A13995, 1976.
16. G. I. BELL AND S. GLASSTONE, "Nuclear Reactor Theory," Chap. 1, Van Nostrand–Reinhold, New York, 1970.